A study of the phosphate mineral kapundaite $NaCa(Fe^{3+})_4(PO_4)_4$ $(OH)_3 \cdot 5(H_2O)$ using SEM/EDX and vibrational spectroscopic methods

Ray L. Frost [a],*, Andrés López [a], Yunfei Xi [a], Ricardo Scholz [b]

[a] School of Chemistry, Physics and Mechanical Engineering, Science and Engineering Faculty, Queensland University of Technology, GPO Box 2434, Brisbane, Queensland 4001, Australia
[b] Geology Department, School of Mines, Federal University of Ouro Preto, Campus Morro do Cruzeiro, Ouro Preto, MG 35 400-00, Brazil

HIGHLIGHTS

- The kapundaite sample originated from the Sapucaia mine a lithium-bearing pegmatite.
- Kapundaite is a hydrated hydroxyl sodium calcium ferric phosphate $NaCa(Fe^{3+})_4(PO_4)_4(OH)_3 \cdot 5(H_2O)$.
- The molecular structure of kapundaite was assessed by vibrational spectroscopy.
- Multiple phosphate bands are observed.

GRAPHICAL ABSTRACT

ABSTRACT

Vibrational spectroscopy enables subtle details of the molecular structure of kapundaite to be determined. Single crystals of a pure phase from a Brazilian pegmatite were used. Kapundaite is the Fe^{3+} member of the wardite group. The infrared and Raman spectroscopy were applied to compare the structure of kapundaite with wardite. The Raman spectrum of kapundaite in the 800–1400 cm^{-1} spectral range shows two intense bands at 1089 and 1114 cm^{-1} assigned to the v_1 PO_4^{3-} symmetric stretching vibrations. The observation of two bands provides evidence for the non-equivalence of the phosphate units in the kapundaite structure. The infrared spectrum of kapundaite in the 500–1300 cm^{-1} shows much greater complexity than the Raman spectrum. Strong infrared bands are found at 966, 1003 and 1036 cm^{-1} and are attributed to the v_1 PO_4^{3-} symmetric stretching mode and v_3 PO_4^{3-} antisymmetric stretching mode. Raman bands in the v_4 out of plane bending modes of the PO_4^{3-} unit support the concept of non-equivalent phosphate units in the kapundaite structure.

In the 2600–3800 cm^{-1} spectral range, Raman bands for kapundaite are found at 2905, 3151, 3311, 3449 and 3530 cm^{-1}. These bands are broad and are assigned to OH stretching vibrations. Broad infrared bands are also found at 2904, 3105, 3307, 3453 and 3523 cm^{-1} and are attributed to water. Raman spectroscopy complimented with infrared spectroscopy has enabled aspects of the structure of kapundaite to be ascertained and compared with that of other phosphate minerals.

© 2013 Elsevier B.V. All rights reserved.

Introduction

Kapundaite [1,2] is a hydrated hydroxyl sodium calcium ferric phosphate $NaCa(Fe^{3+})_4(PO_4)_4(OH)_3 \cdot 5(H_2O)$. The mineral is structurally related to mélonjosephite [3]. Kapundaite is known from Tom's phosphate quarry, Kapunda, South Australia, Australia. This locality is a wonderful source of phosphate minerals. Other minerals from this locality are natrodufrenite, meurigite-Na and leucophosphite.

The crystal structures of kapundaite have been solved [1,2]. The mineral crystallize with triclinic symmetry. The cell dimensions

* Corresponding author. Tel.: +61 7 3138 2407; fax: +61 7 3138 1804.
E-mail address: r.frost@qut.edu.au (R.L. Frost).

are *Space Group*: P-1, $a = 6.317(5)$ Å, $b = 7.698(6)$ Å, $c = 19.04(1)$ Å, $\alpha = 105.53(1)°$, $\beta = 99.24(2)°$, $\gamma = 90.09(2)°$, $V = 451.2(6)$ Å^3 and $Z = 1$. The structure of kapundaite is based on a unique corrugated octahedral–tetrahedral sheet parallel to [0 0 1]. The Na/Ca site between the sheets is 8-coordinated, with three Na/Ca–O bonds to one sheet and one Na/Ca–O bond to the other sheet. The remaining four Na/Ca–O bonds are to H_2O molecules. The octahedral–tetrahedral sheet is composed of two types of chains parallel to the *a* direction. One chain consists of trans-edge-sharing octahedral decorated by PO_4 linking free vertices of adjacent octahedral in a staggered arrangement [1,2].

To the best knowledge of the authors, this work reports the first vibrational spectroscopic study of kapundaite. Due to similar composition, the results will be compared with minerals of the wardite group. Tarte et al. collected the infrared spectra of five samples of cyrylovite and wardite. Between wardite's composition, $NaAl_3$ $(PO_4)_2(OH)_4 \cdot 2(H_2O)$, and kapundaite's composition, $NaCa(Fe^{3+})_4$ $(PO_4)_4(OH)_3 \cdot 5(H_2O)$, these minerals are able to form end members of a series of solid solutions. Either of the two minerals can occur in various proportions in a series of solid solutions in the wardite mineral group. Kapundaite is a rare accessory mineral in some oxidizing phosphate-bearing granite pegmatites and iron deposits.The vibrational spectrum is dependent upon the ratio of the Ca/Fe. Tarte et al. found that the two minerals wardite and cyrilovite can be distinguished by the spectral patterns of the OH stretching region in the infrared spectrum [4]. These workers did not interpret the spectra of the phosphate because of complexity and no detailed assignment was given. Breitinger et al. [5] reported the combined vibrational spectra of a natural wardite. Breitinger and co-workers used a full array of techniques including inelastic neutron scattering, infrared, Raman and near infrared techniques [5]. These workers used a natural wardite with significant amounts of ferric iron in the structure. In other words the sample analyzed was fundamentally a solid solution of wardite and kapundaite, but at the wardite end. The original papers on the infrared spectrum of isolated phosphate units was published by Lazarev [6]. Of course, phosphates structures are different. Usually they have rather low symmetry: orthorhombic, monoclinic, or even triclinic [7]. Farmer based upon the work of Petrov et al. [8–10] made a comparison of the results of the vibrational spectrum of a series of phosphates.

Raman spectroscopy has proven very useful for the study of minerals [11–15]. Indeed, Raman spectroscopy has proven most useful for the study of diagenetically related minerals where isomorphic substitution may occur as with wardite, cyrilovite and kapundaite, as often occurs with minerals containing phosphate groups. This paper is a part of systematic studies of vibrational spectra of minerals of secondary origin in the pegmatite rocks. The objective of this research is to report the Raman and infrared spectra of kapundaite and to relate the spectra to the molecular structure of the mineral.

Experimental

Samples description and preparation

The kapundaite sample studied in this work was obtained from the collection of the Geology Department of the Federal University of Ouro Preto, Minas Gerais, Brazil, with sample code SAC-111. Kapundaite sample studied in this work is from the Tom's quarry, Austrália and can be considered a type material. The sample was gently crushed and the associated minerals were removed under a stereomicroscope Leica MZ4. The kapundaite sample was phase analyzed by X-ray diffraction. Scanning electron microscopy (SEM) in the EDS mode was applied to support the mineral characterization.

Raman spectroscopy

Crystals of kapundaite were placed on a polished metal surface on the stage of an Olympus BHSM microscope, which is equipped with 10×, 20×, and 50× objectives. The microscope is part of a Renishaw 1000 Raman microscope system, which also includes a monochromator, a filter system and a CCD detector (1024 pixels). The Raman spectra were excited by a Spectra-Physics model 127 He–Ne laser producing highly polarised light at 633 nm and collected at a nominal resolution of 2 cm^{-1} and a precision of ±1 cm^{-1} in the range between 200 and 4000 cm^{-1}. Some of these mineral fluoresced badly at 633 nm; as a consequence other laser excitation wavelengths were used especially the 785 nm laser. Repeated acquisitions on the crystals using the highest magnification (50×) were accumulated to improve the signal to noise ratio of the spectra. Spectra were calibrated using the 520.5 cm^{-1} line of a silicon wafer. Previous studies by the authors provide more details of the experimental technique. Alignment of all crystals in a similar orientation has been attempted and achieved. However, differences in intensity may be observed due to minor differences in the crystal orientation.

Infrared spectroscopy

Infrared spectra were obtained using a Nicolet Nexus 870 FTIR spectrometer with a smart endurance single bounce diamond ATR cell. Spectra over the 4000–525 cm^{-1} range were obtained by the co-addition of 128 scans with a resolution of 4 cm^{-1} and a mirror velocity of 0.6329 cm/s. Spectra were co-added to improve the signal to noise ratio.

Spectral manipulation such as baseline correction/adjustment and smoothing were performed using the Spectracalc software package GRAMS (Galactic Industries Corporation, NH, USA). Band component analysis was undertaken using the Jandel 'Peakfit' software package that enabled the type of fitting function to be selected and allows specific parameters to be fixed or varied accordingly. Band fitting was done using a Lorentzian-Gaussian cross-product function with the minimum number of component bands used for the fitting process. The Gaussian–Lorentzian ratio was maintained at values greater than 0.7 and fitting was undertaken until reproducible results were obtained with squared correlations of r^2 greater than 0.995.

Results and discussion

Chemical characterization

The SEM image of kapundaite sample studied in this work is shown in the supplementary information as Fig. S1. Kapundaite crystals show a prismatic to tabular habitus and the crystal forms a reticular aggregate. Qualitative chemical composition shows a homogeneous phase, composed by Na, Ca, Fe and P, with minor amounts of Al (Fig. 1). The sample can be considered a pure phase.

Spectroscopy

The Raman spectrum of kapundaite in the 100–4000 cm^{-1} spectral range is illustrated in Fig. 2a. This spectrum shows the position of the Raman bands and their relative intensities. It is obvious that there are large parts of the spectrum where little or no intensity is observed. Therefore, the spectrum is subdivided into sections according to the type of vibration being investigated. In this way the precise position of the bands can be detailed. The infrared spectrum of kapundaite in the 500–4000 cm^{-1} spectral range is shown in Fig. 2b. The reflectance spectrum starts at 500 cm^{-1} because the
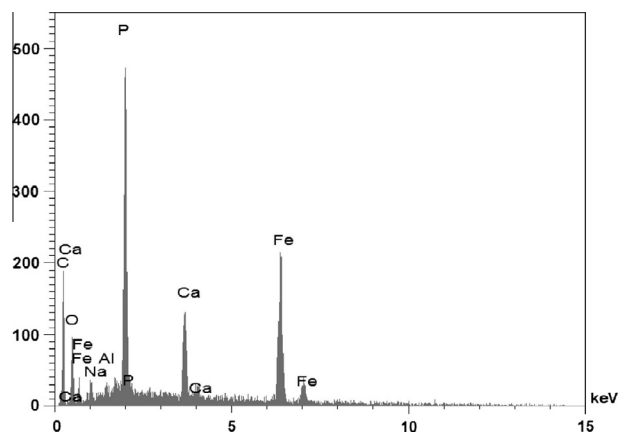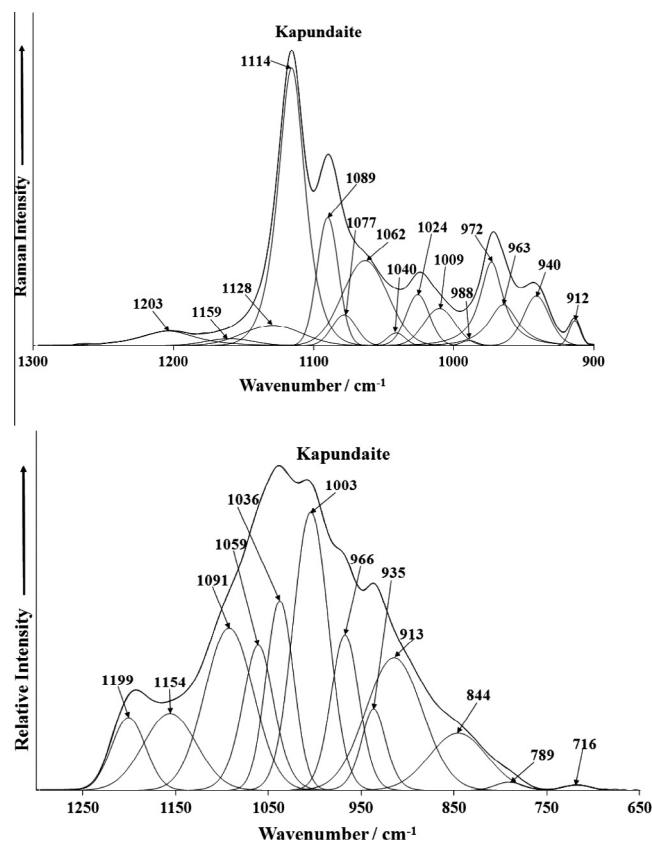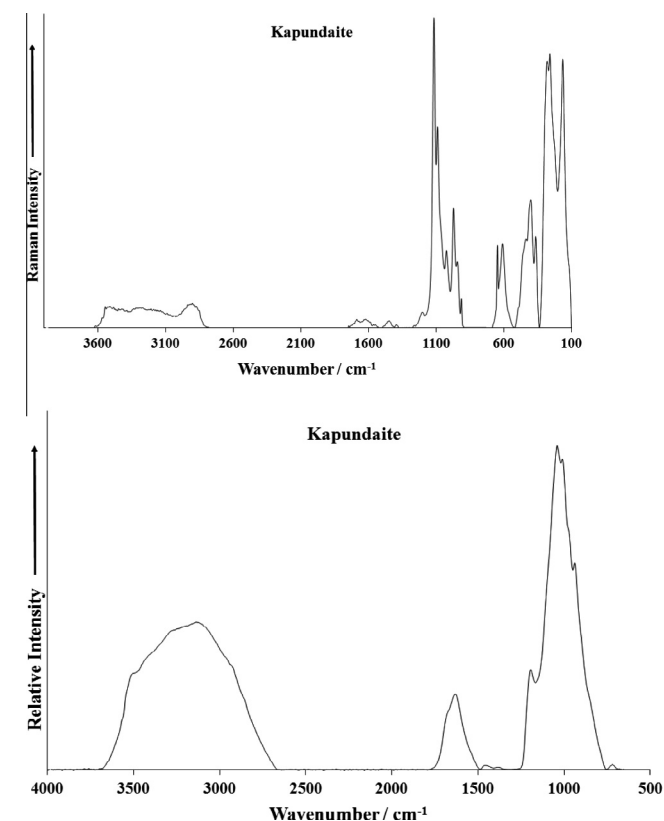
Fig. 1. EDS spectra of kapundaite.

Fig. 2. (a) Raman spectrum of kapundaite over the 100–4000 cm^{-1} spectral range and (b) infrared spectra of kapundaite over the 500–4000 cm^{-1} spectral range.

Fig. 3. (a) Raman spectrum of kapundaite over the 800–1400 cm^{-1} range and (b) Infrared spectrum of kapundaite over the 500–1300 cm^{-1} range.

ATR cell absorbs all infrared radiation below this wavenumber. As for the Raman spectrum, the infrared spectrum is subdivided into sections depending upon the type of vibration being examined. The complete infrared spectrum displays the position of the infrared bands and their relative intensity.

The Raman spectrum of kapundaite in the 900–1300 cm^{-1} spectral range is reported in Fig. 3a. The Raman spectrum is dominated by two intense bands at 1089 and 1114 cm^{-1}. These two bands are assigned to the v_1 PO$_4^{3-}$ symmetric stretching vibrations. Two intense bands are observed reflecting two non-equivalent phosphate units in the kapundaite structure. A comparison may be made with the spectrum of wardite. The Raman spectrum of wardite is dominated by two intense bands at around 995 and 1051 cm^{-1}. The spectra appear to differ considerably from that obtained by

Breitinger et al. [5]. Breitinger et al. used FT-Raman to obtain their spectrum and found overlapping Raman bands at 999 and 1033 cm^{-1} and assigned these bands to the v_1 PO$_4^{3-}$ symmetric stretching and v_3 PO$_4^{3-}$ antisymmetric stretching modes. The difference in the spectra between our work and that of Breitinger et al., may be attributed to the improved technology of the Raman spectrometer with greater resolution. The Raman spectrum (Fig. 3a) shows a resolved component band at 1024 cm^{-1}. There is also a band at 972 cm^{-1}. Breitinger et al. [5] also assigned the band at 999 cm^{-1} to AlOH deformation modes. In this work the band at 972 cm^{-1} is very sharp and well resolved.

A series of low intensity bands are noted at 1128, 1159 and 1203 cm^{-1}. These bands are assigned to the v_3 PO$_4^{3-}$ antisymmetric stretching modes. The Raman spectrum of wardite shows a group of low intensity bands are observed at 1084, 1108, 1120, 1140 and 1186 cm^{-1}. Breitinger et al. [5] did not report any bands in these positions in the Raman spectrum of synthetic wardite. These researchers reported infrared bands at 1058 (strong) with shoulders at 1129 and 1168 cm^{-1} and assigned these bands to δAl$_2$OH deformation modes. A low intensity broad band at 884 cm^{-1} (a), 902 cm^{-1} (b) and 893 cm^{-1} (c) are assigned to a water librational mode. In the work of Breitinger et al. [5] a broad low intensity band was found at around 800 cm^{-1} and was attributed to water librational modes. In the Raman spectrum of kapundaite two component bands are observed at 811 and 852 cm^{-1}. These bands may be attributed to the water librational modes. Normally the intensity of water librational modes are of a quite low intensity in the Raman spectrum but may show significantly greater intensity in the infrared spectrum.

The infrared spectrum of kapundaite in the 6501300 cm^{-1} spectral range is shown in Fig. 3b. The infrared spectrum of kapundaite shows much greater complexity than the Raman spectrum. It is

noted that the two infrared bands at 844 and 913 cm^{-1} attributed to the water librational modes show much greater intensity. Strong infrared bands are found at 935, 966, 1003, 1036, 1059, 1091 and 1199 cm^{-1} and are attributed to the v_1 PO$_4^{3-}$ symmetric and anti-symmetric stretching modes. The observation of these bands supports the concept that the phosphate units in the kapundaite structure are not equivalent. The series of infrared bands between 1036 and 1199 cm^{-1} are assigned to the v_3 PO$_4^{3-}$ antisymmetric stretching modes. In the infrared spectrum of wardite, bands are observed at 1039, 1056, 1069, 1084, 1102, 1135 and 1165 cm^{-1}. Some of these bands may also be due to the δAl$_2$OH deformation modes, in harmony with the assignment of Breitinger et al. He and his co-workers stated that the deceptively simple strong IR band centered at 1059 cm^{-1} contains at least four components of v(PO$_4$) generated by lifting of the originally threefold degeneracy of v_3(PO$_4$) and activation of v_1(PO$_4$) due to the general position of PO$_4$ and again at least four components of the deformation modes δ(Al$_2$OH) involving the two pairs of the non-equivalent OH groups. In this work we have obtained much greater resolution and these components are resolved into the component bands.

The Raman spectrum of kapundaite in the 350–700 cm^{-1} spectral range and in the 100–350 cm^{-1} spectral range are displayed in Fig. 4a and b. Raman bands are observed at 609 and 646 cm^{-1} and are assigned to the v_4 out of plane bending modes of the PO$_4^{3-}$ units. In the Raman spectrum of wardite, bands are observed at 605 and 618 cm^{-1} with shoulders at 578 and 589 cm^{-1}. Breitinger et al. assigned these bands to v(Al(O/OH)$_6$) stretching vibrations. No phosphate bending modes in the work of Breitinger et al. were reported. The Raman spectrum of crystalline NaH$_2$PO$_4$ shows Raman bands at 526, 546 and 618 cm^{-1} (data obtained by the authors). A series of Raman bands for kapundaite at 395, 412, 435, 460 and 491 cm^{-1} are observed. These bands are attributed

to the v_2 PO$_4^{3-}$ and H$_2$PO$_4$ bending modes. A comparison may again be made with the Raman spectrum of wardite. The series of Raman bands at 388, 400, 455, 478 and 502 cm^{-1} for wardite are attributed to the v_2 PO$_4^{3-}$ bending modes. Raman bands at 317, 446 and 515 cm^{-1} for wardite reported by Breitinger et al. [5] were assigned to vibrational modes of the AlO$_6$/AlOH$_6$ units. However, this assignment differs from that reported in this work. An intense Raman band is observed at 361 cm^{-1} and is denoted as a CaO stretching vibration (Fig. 4a). Strong Raman bands are observed at 257, 275 and 295 cm^{-1}. Intense Raman bands for wardite observed at 258 cm^{-1} are thought to be related to the O–Al–O skeletal stretching vibrations. Other Raman bands for kapundaite are observed at 113, 137, 162 and 186 cm^{-1}. These bands are simply described as external vibrations.

The Raman spectrum of kapundaite in the 2700–3700 cm^{-1} spectral range is displayed in Fig. 5a. The infrared spectrum of kapundaite in the 2500–3800 cm^{-1} is reported in Fig. 5b. Strong Raman bands for kapundaite are found at 2905, 3449 and 3530 cm^{-1} with a broad bands at 3151 and 3311 cm^{-1}. These bands are assigned to OH stretching vibrations. In the infrared spectrum (Fig. 5b), strong infrared bands are observed at 3105, 3307, 3453 and 3523 cm^{-1}. The infrared spectrum shows broad bands. Tarte et al. reported the infrared spectrum of wardite and cyrilovite. They found that O–H stretching wavenumbers are distributed into 2 spectra regions: 2 very broad bands near 2950 and 3300 cm^{-1}, which are due to H$_2$O molecules engaged in short H bonds; and 2 very sharp and strong peaks (3550 and 3495 cm^{-1} for pure cyrilovite, 3621 and 3555 cm^{-1} for pure wardite) due to the stretch of hydroxyl group. Sharp infrared bands for wardite are observed at 3544 and 3611 cm^{-1} and are attributed to the OH stretching vibrations of the hydroxyl units. A sharp band in the infrared spectrum is observed at 3480 cm^{-1} for the sample
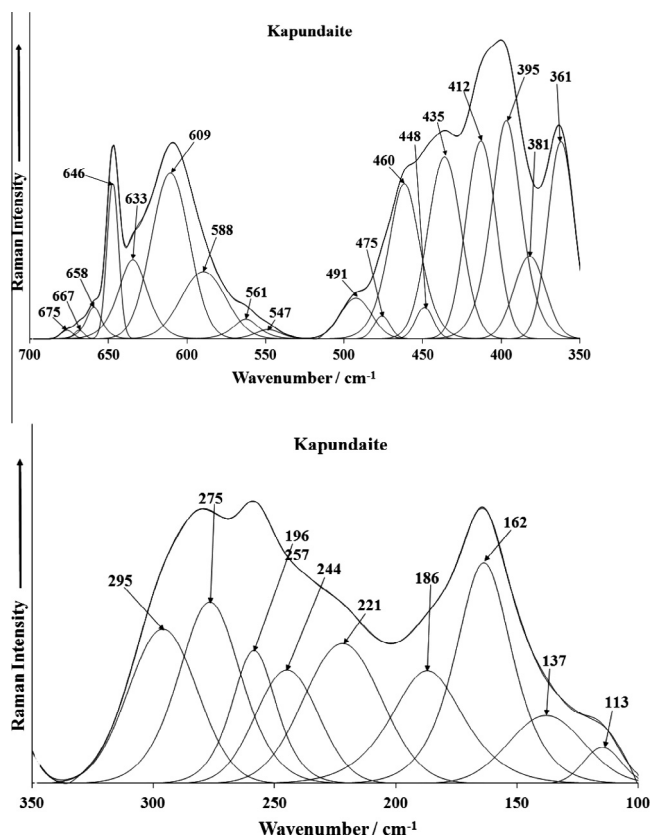

Fig. 4. (a) Raman spectrum of kapundaite over the 300–800 cm^{-1} range and (b) Raman spectrum of kapundaite over the 100–300 cm^{-1} range.
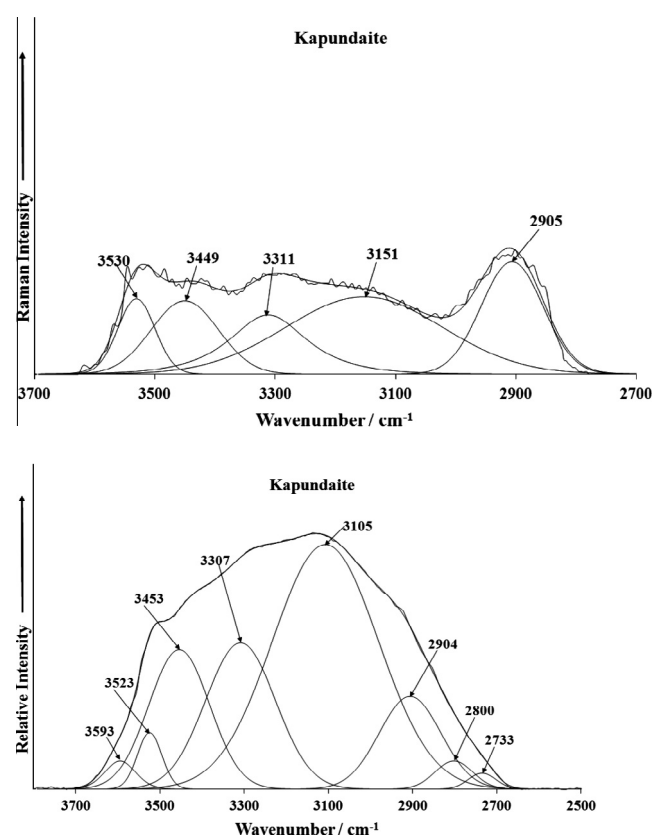

Fig. 5. (a) Raman spectrum of kapundaite over the 2600–3800 cm^{-1} spectral range and (b) Infrared spectrum of kapundaite over the 2400–3800 cm^{-1} range.
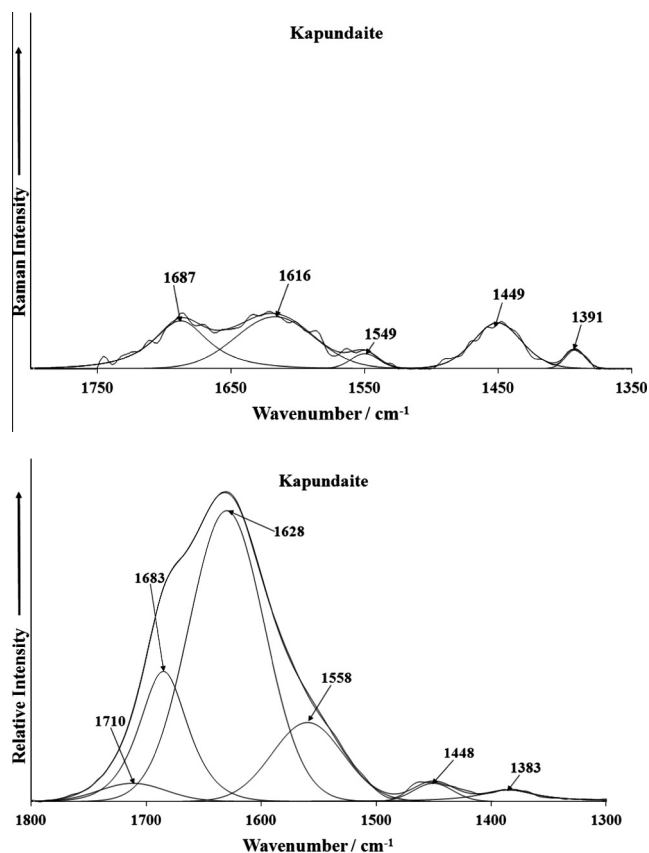
Fig. 6. (a) Raman spectrum of kapundaite over the 1400–1800 cm^{-1} spectral range and (b) Infrared spectrum of kapundaite over the 1300–1900 cm^{-1} range.

from Utah. This band may be due to FeOH stretching vibrations. Breitinger et al. [5] found infrared bands at 3520 (vw), 3545 (s), 3585 (sh) and 3613 cm^{-1} (m). Breitinger et al. states that the v(OH) modes in the two independent pairs of symmetry-correlated OH groups classify as 2a + 2b; with the correlation splitting between a and b species depending on the distances in each of the pairs [5]. The v(OH) region of IR spectra of wardite shows two sharp bands (3613 and 3545 cm^{-1}) with two weak shoulders or satellites (3580 and 3520 cm^{-1}). It is likely that the two sharp infrared bands are due to two independent and non-equivalent OH units. The two sharp shoulder bands may be attributed to the Al–OH–Fe groups. Broad infrared bands are observed at 2876 and 3268 cm^{-1} are assigned to water stretching vibrations. It is probable that some of the component bands are due to overtones and combination of the water bending and librational modes. The position of the water stretching vibration provides evidence for strong hydrogen bonding and that water is involved in different hydrogen bonding arrangements. The band at around 2893 cm^{-1} gives an indication that water is very strongly hydrogen bonded in the kapundaite structure.

The Raman spectrum of kapundaite in the 1350–1800 cm^{-1} spectral range is illustrated in Fig. 6a. The spectrum suffers from a lack of signal; this is not unusual as water is a very weak Raman scatterer. Raman bands are observed at 1599 and 1634 cm^{-1}. These bands are assigned to water bending modes. In contrast, the infrared spectrum of kapundaite is displayed in Fig. 6b, where significant intensity is observed. Water is a very strong infrared absorber. Infrared bands are observed at 1599 and 1650 cm^{-1} and are assigned to water bending modes. Infrared bands for

wardite are observed at 1549, 1670 and 1748 cm^{-1}. The bands in this region result from correlation splitting as a result of the short distance and orientation of the H_2O molecules. Additional bands for wardite are observed at 1417 and 1476 cm^{-1}. The assignment of these bands is due to OH deformation modes. The presence or absence of these bands depends upon the Fe/Al ration in the kapundaite/wardite mineral samples.

Conclusions

Kapundaite [1,2] is a hydrated hydroxyl sodium calcium ferric phosphate NaCa(Fe^{3+})$_4$(PO$_4$)$_4$(OH)$_3$·5(H$_2$O). The mineral is structurally related to mélonjosephite [3].

Raman spectroscopy complimented with infrared spectroscopy has been used to study aspects of the molecular structure of the mineral kapundaite. The structure of kapundaite is triclinic. As a consequence multiple phosphate vibrational modes are observed. Raman and infrared bands are observed and attributed to phosphate, hydroxyl and water vibrational stretching and bending modes.

Acknowledgments

Appendix A. Supplementary material

Supplementary data associated with this article can be found, in the online version, at http://dx.doi.org/10.1016/j.saa.2013.11.020.

References

[1] S.J. Mills, W.D. Birch, A.R. Kampf, A.G. Christy, J.J. Pluth, A. Pring, M. Raudsepp, Y.-S. Chen, Am. Min. 95 (2010) 754–760.
[2] S.J. Mills, U. Kolitsch, R. Miyawaki, F. Hatert, G. Poirier, A.R. Kampf, S. Matsubara, E. Tillmanns, Euro. J. Min. 22 (2010) 595–604.
[3] A.M. Fransolet, Bull. Soc. Fr. Min. 96 (1973) 135–142.
[4] P. Tarte, A.M. Fransolet, F. Pillard, Bull. Min. 107 (1984) 745–754.
[5] D.K. Breitinger, H.H. Belz, L. Hajba, V. Komlosi, J. Mink, G. Brehm, D. Colognesi, S.F. Parker, R.G. Schwab, J. Mol. Struct. 706 (2004) 95–99.
[6] A.N. Lazarev, Kolebatielnyje Spektry I Strojenije Silikatov, Nauka, Leningrad, 1968.
[7] W. Jastrzebski, M. Sitarz, M. Rokita, K. Bulat, Spectrochim. Acta A 79 (2011) 722–727.
[8] I. Petrov, B. Soptrajanov, N. Fuson, Zeit. Anorgan. Allg. Chem. 358 (1968) 178–186.
[9] I. Petrov, B. Soptrajanov, N. Fuson, J.R. Lawson, Spectrochim. Acta A 23 (1967) 2637–2646.
[10] K.I. Petrov, I.V. Tananaev, V.G. Pervykh, S.M. Petushkova, Zh. Neorgan. Khimii. 12 (1967) 2645–2650.
[11] R.L. Frost, Y. Xi, R. Scholz, M. Belotti Fernanda, Spectrochim. Acta A 103 (2013) 143–150.
[12] R.L. Frost, Y. Xi, R. Scholz, M. Belotti Fernanda, A. Dias Menezes Filho Luiz, Spectrochim. Acta A 104 (2013) 250–256.
[13] R.L. Frost, A. Lopez, Y. Xi, A. Granja, R. Scholz, R.M.F. Lima, Spectrochim. Acta A 114 (2013) 309–315.
[14] R.L. Frost, Y. Xi, M. Beganovic, F.M. Belotti, R. Scholz, Spectrochim. Acta A 107 (2013) 241–247.
[15] R.L. Frost, Y. Xi, R. Scholz, Spectrochim. Acta A 108 (2013) 244–250.